Two approaches to three-dimensional array foci of generalized Fibonacci structures

Jie Ke (柯 杰)[1,2], Junyong Zhang (张军勇)[1,*], and Zhiyuan Ren (任志远)[1]

[1]*National Laboratory on High Power Laser and Physics, Shanghai Institute of Optics and Fine Mechanics, Chinese Academy of Sciences, Shanghai 201800, China*

[2]*University of Chinese Academy of Sciences, Beijing 100049, China*

**Corresponding author: zhangjin829@163.com*

Received January 24, 2016; accepted March 25, 2016; posted online April 28, 2016

We propose two technologies to extend the number of layers in order to complete the three-dimensional (3D) array diffraction-limited foci, which means there are two-dimensional array foci at multi-focal planes. One technology is the diffractive optical lever; the other is multi-hybrid Fibonacci structures. Based on the aperiodic Fibonacci structures and binary phase modulation, various kinds of devices can be designed to produce 3D array foci whose focusing properties approximately satisfy the mathematical characteristics of the Fibonacci sequences. With those technologies, the diffraction-limited array foci are freely designed or distributed as required at the desired multiple focal planes.

OCIS codes: 050.1965, 080.2720, 220.4000, 340.7480.

doi: 10.3788/COL201614.060501.

Three-dimensional (3D) array foci, as the name implies, mean that two-dimensional (2D) array diffraction-limited foci are distributed as required at multi-focal planes. The focusing and imaging of light have many applications in ophthalmology, biological cell, virtual display techniques, high-resolution microscopy, spectroscopy, and lithography[1]. Unfortunately, a conventional refractive lens cannot focus soft x rays and extreme ultraviolet (EUV) as a consequence of the strong absorption of solid materials in the x ray and EUV spectral regions. Although a traditional Fresnel zone plate (FZP) can be used for this kind of focusing[2–4], it has inherent limitations[5–7]. Some aperiodic zone plates generated by the fractal Cantor set have been proposed to overcome these limitations[8–10]. In 2001, a new concept, a photon sieve (PS), was proposed[11]: it is an FZP with the transparent zones replaced by a great number of completely separated pinholes to overcome the disadvantages of traditional zone plates. Then many kinds of PSs were designed and studied in detail[12–19].

Actually, there is only one focus at a single focal plane, whether one is using an FZP or PSs. In 2013, an aperiodic Fibonacci sequence was introduced into planar diffractive optical elements (DOEs) and generated two foci with a definite relationship along the optical axis[20–25]. The other interesting array illuminator is the Dammann grating[26–28], but it can only focus light in the far field. We find that the former functionality is achieved by a quasi-periodic structure, but the latter Dammann grating is a periodic structure. In our previous work, we proposed a generalized Fibonacci PS and produced two adjustable foci on-axis according to the mathematical character of generalized Fibonacci sequences[24]. This technology can produce multiple foci on the optical axis.

In this Letter, we propose another two approaches to extend the basic Fibonacci structures so as to get more than two layers. One is the diffractive optical lever; the other is multi-hybrid Fibonacci sequences. By means of proper encoding and binary phase modulation, the Fibonacci structure does generate the 3D diffraction-limited array foci. That means a single planar DOE can focus light into multiple foci with different coordinates in 3D space.

For the generalized Fibonacci sequences, the initial seeds and the corresponding linear recursion relation are given by

$$\begin{cases} F_1 = a, F_2 = b, (a, b \in N) \\ F_n = pF_{n-1} + qF_{n-2}, (p, q \in N, n \geq 3, n \in N) \end{cases}. \tag{1}$$

The absolute value of one of the corresponding characteristic roots of the recursion relation can be defined as the limit of the ratio of two consecutive generalized Fibonacci numbers:

$$\gamma = \lim_{j \to \infty} F_j / F_{j-1}. \tag{2}$$

When $(p, q) = (1, 1)$, we can get the standard Fibonacci sequence. The characteristic equation is $\gamma^2 - \gamma - 1 = 0$, and the corresponding characteristic roots are -0.6180 and 1.6180 and are called the golden mean. If (p, q) are set to other values, it denotes the other generalized Fibonacci sequences, whose characteristic roots are called the generalized golden mean.

The optical path difference between two adjacent zones is equal to 0.5λ, where λ is the incident wavelength. If 0.5λ is replaced with $K\lambda(K > 0)$, where K denotes the optical path difference scaling factor (OPDSF), we can get the diffractive optical lever[24]. The diffracted field can be calculated by the Rayleigh–Sommerfeld diffraction integral:

$$E_1(x,y,z)=\frac{-1}{2\pi}\iint E_0(\xi,\eta,0)t(\xi,\eta)\frac{\partial}{\partial z}\left[\frac{\exp(ikR)}{R}\right]\mathrm{d}\xi\mathrm{d}\eta, \tag{3}$$

where $R=[(x-\xi)^2+(y-\eta)^2+z^2]^{1/2}$, $E_0(\xi,\eta,0)$ denotes the incident light, and $t(\xi,\eta)$ is the corresponding transmission function of each transparent region. According to the linear superposition principle, the total diffracted field of the generalized Fibonacci structures is the simple sum of those individual diffracted fields from different regions.

Figure 1 shows the schematic of aperiodic structure with switching (010010100100101), where zero denotes the opaque zones, while one denotes the transparent ones. The red denotes the zero phase, and the blue denotes the π phase.

Taking the standard Fibonacci with an encoded seed $(F^1,F^2)=(01,010)$ into account, for a polar Fibonacci structure, the transparent zones are set to the zero phase if the polar radius of the zone is less than 0.574 times the radius of the device; otherwise, the transparent zones are set to the π phase. A monochromatic plane wave with wavelength λ of 632.8 nm is incident on the optical structure, and the expected focal length f_0 is 3.5 cm. In this case, second-order annular spots can be obtained, as shown in Fig. 2. For a Cartesian Fibonacci structure, the transparent zone is set to the zero phase if the absolute value of the center of the zone is less than 0.501 times the half-width of device; otherwise, the transparent zone is set to the π phase. The intensity contour in 3D space is displayed in Fig. 3. Figure 3 indicates that the Cartesian Fibonacci device does generate 2×2 array foci at two focal planes. The two sets of focal planes are all located at $f_2=2.830$ cm and $f_1=4.584$ cm. They all have the same 89 transparent zones and 144 opaque zones. In Figs. 2 and 3, all the focal spots are diffraction limited. The ratios of the sizes of the spots at the two focal planes are approximately equal to the ratios of the distances between their own focal planes and the generalized Fibonacci structures.

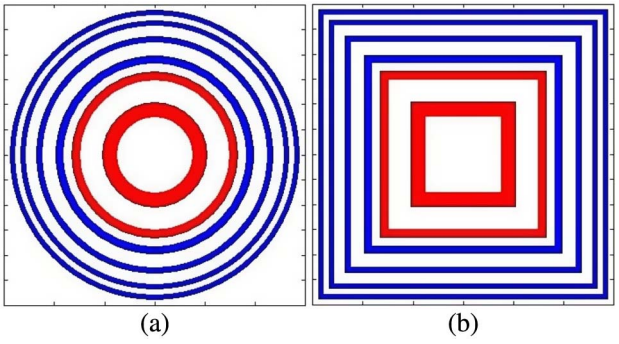

Fig. 1. Fibonacci structure unit (a) in polar coordinates and (b) in Cartesian coordinates.

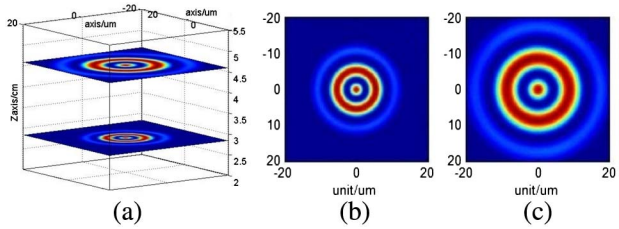

Fig. 2. Intensity contours at two focal planes against a polar Fibonacci structure (a) in 3D space, (b) at the first focal plane, and (c) at the second focal plane.

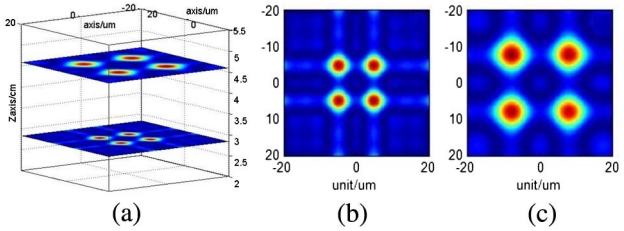

Fig. 3. Intensity contours at two focal planes against a Cartesian Fibonacci structure (a) in 3D space, (b) at the first focal plane, and (c) at the second focal plane.

In order to obtain more than two-layer array foci, two different technologies are proposed. First, we investigate the first technology: the diffraction optical lever. Here, the analytical expression of the distance between the device and the focal planes can be given by[25]:

$$f_m=\frac{f_0\times K}{\left[\frac{m-1}{2}\right]+\begin{vmatrix}\mathrm{mod}(m-1,2) & -\mathrm{mod}(m,2)\\ (\gamma+1)^{-1} & \gamma^{-1}+1\end{vmatrix}},\quad f_m<\cdots<f_1, \tag{4}$$

where $[x]$ denotes the nearest integers less than or equal to x, $\mathrm{mod}(X,2)$ represents the modulus after division 2, m denotes the mth layer, f_0 is the expected focal length, and K is the OPDSF.

We again take the standard Fibonacci as an example. The schematic is shown in Fig. 4(a). The incident wavelength and the expected focal length remain the same. The Fibonacci structure has 144 transparent zones and 233 opaque zones and is divided into two regions along the radial direction. The inner region is from the first zone to the 200th zone and is set to the spiral phase from zero to π. The outer region is from the 201st zone to the

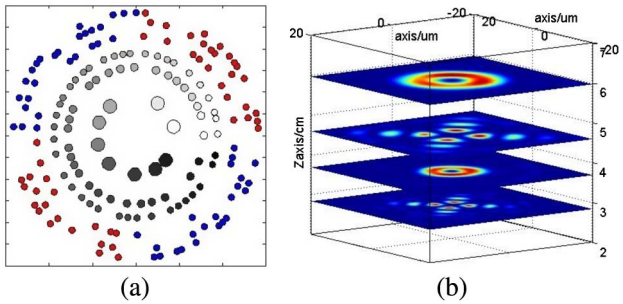

Fig. 4. (a) A Fibonacci structure based on the diffractive optical lever. (b) Intensity contours at four focal planes in 3D space.

377th zone and is divided into four quadrants which are, in order, $(0, 0.5\pi]$, $(0.5\pi, \pi]$, $(\pi, 1.5\pi]$, and $(1.5\pi, 2\pi]$. The red pinhole denotes the zero phase, and the blue pinhole denotes the π phase. The OPDSF in the inner region is equal to 0.50, and the OPDSF in the outer region is 0.65. The distance between the device and the focal planes with respect to the outer region is 0.65/0.50 times the focal lengths produced by the inner region. In this way, the four-layer array foci can be obtained as indicated in Figs. 4(b) and 5. The focal planes are located at 2.830, 3.679, 4.584, and 5.959 cm. There are hollow spots at the second and the fourth focal planes. At the first and third focal planes, it presents array foci.

The other technology involves making the most of multi-hybrid Fibonacci sequences. Figure 6(a) shows the schematic of this structure. In this case, $\lambda = 632.8$ nm and $f_0 = 3.5$ cm. The structure is also divided into four equal regions along the Cartesian coordinates. The first and the third quadrants correspond to the standard Fibonacci sequence and have 89 transparent zones and 144 opaque zones. The second and the fourth quadrants correspond to the generalized Fibonacci sequence with $(p, q) = (-2, 0.3)$ and have 77 transparent zones and 164 opaque zones. They have the same encoded seeds $(F^1, F^2) = (01, 010)$. The value 0 still denotes the opaque pinhole, but the transparent pinhole is completely replaced with phase modulation. The phases are, in order, $\pi/2$, π, $3\pi/2$, and 2π in each region. The four intervals are, in order, $(0, \pi/2]$, $(\pi/2, \pi]$, $(\pi, 3\pi/2]$, and $(3\pi/2, 2\pi]$. There are two focal spots at each focal plane, and the two focal spots along the angle of 45° are mainly produced by the first and the third quadrants, and at another two focal planes, there are two focal spots along the angle of 135° mainly produced by the second and the fourth quadrants. With this technology, we produce

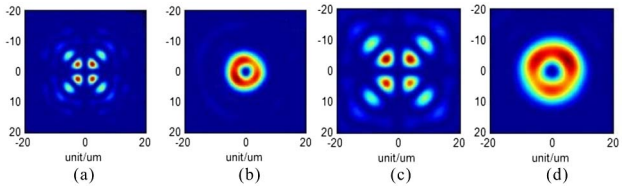

Fig. 5. Intensity contours at four focal planes compared against Fig. 4(a).

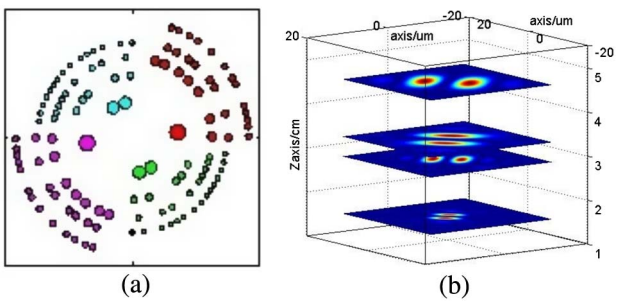

Fig. 6. (a) A multi-hybrid Fibonacci structure. (b) Intensity contours at four focal planes in 3D space.

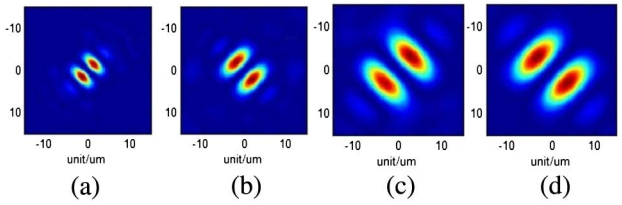

Fig. 7. Intensity contours at four focal planes compared against Fig. 6(a).

the four-layer array foci. The four focal planes are located at 1.53, 2.83, 3.28, and 4.58 cm. Obviously, the four focal planes satisfy the relation $f_2 - f_1 = f_4 - f_3$. It is more important that the former two focal spots are orthogonal to the latter two focal spots, as shown in Figs. 6(b) and 7, which give the intensity contours at the four focal planes.

Different from traditional FZPs or PSs with a single spot and the Dammann grating with array foci only in the far-field plane, the aperiodic Fibonacci structures can be used to produce 3D array diffraction-limited foci from the near field to the far field. When the transparent zones are replaced with some pinholes, it is convenient to adjust the transmittance of each region so as to control the intensity at each focal plane. The diffractive optical lever can double the layers only by one sequence, while the multi-hybrid structure can increase the layers by more than one aperiodic sequence. By using them, we are free to design various kinds of multifocal nanophotonic devices with any number and at any location. The generalized Fibonacci structures can offer many applications in x ray microscopes, lithography, biological cells and ophthalmology, and terahertz imaging. Additionally, as the consequence of its outstanding properties, it may be useful for designing generalized quasi-crystals, gratings, and lenses.

This work was supported in part by the National Natural Science Foundation of China under Grant Nos. 61205212 and 61505228.

References

1. F. Zhu, J. Ma, W. Huang, J. Wang, and C. Zhou, Chin. Opt. Lett. **12**, 080501 (2014).
2. E. Champagne, Appl. Opt. **7**, 381 (1968).
3. J. A. Sun and A. Cai, J. Opt. Soc. Am. **8**, 33 (1991).
4. J. Alda, J. M. Rico-García, F. J. Salgado-Remacha, and L. M. Sanchez-Brea, Opt. Commun. **282**, 3402 (2009).
5. D. J. Stiglian, R. Mittra, and R. G. Semonin, J. Opt. Soc. Am. **57**, 610 (1967).
6. M. D. Tipton, J. E. Dowdey, and H. J. Caulfiel, Opt. Eng. **12**, 125166 (1973).
7. H. Kyuragi and T. Urisu, Appl. Opt. **24**, 1139 (1985).
8. G. Saavedra, W. D. Furlan, and J. A. Monsoriu, Opt. Lett. **28**, 971 (2003).
9. J. A. Davis, S. P. Sigarlaki, J. M. Craven, and M. L. Calvo, Appl. Opt. **45**, 1187 (2006).
10. V. Ferrando, A. Calatayud, F. Giménez, W. D. Furlan, and J. A. Monsoriu, Opt. Express **21**, 2701 (2013).

11. L. Kipp, M. Skibowski, R. L. Johnson, R. Berndt, R. Adelung, S. Harm, and T. Seemann, Nature **414**, 184 (2001).
12. Q. Cao and J. Jahns, J. Opt. Soc. Am. A **20**, 1005 (2003).
13. F. Giménez, J. A. Monsoriu, W. D. Furlan, and A. Pons, Opt. Express **14**, 11958 (2006).
14. H.-H. Chung, N. M. Bradman, M. R. Davidson, and P. H. Holloway, Opt. Eng. **47**, 118001 (2008).
15. J. Jia and C. Xie, Chin. Phys. B **18**, 183 (2009).
16. C. Zhou, X. Dong, L. Shi, C. Wang, and C. Du, Appl. Opt. **48**, 1619 (2009).
17. C. Xie, X. Zhu, L. Shi, and M. Liu, Opt. Lett. **35**, 1765 (2010).
18. A. Sabatyan and S. Mirzaie, Appl. Opt. **50**, 1517 (2011).
19. A. Sabatyan and S. A. Hoseini, Appl. Opt. **53**, 7331 (2014).
20. J. A. Monsoriu, A. Calatayud, L. Remón, W. D. Furlan, G. Saavedra, and P. Andrés, IEEE Photon. J. **5**, 3400106 (2013).
21. A. Calatayud, V. Ferrando, L. Remón, W. D. Furlan, and J. A. Monsoriu, Opt. Express **21**, 10234 (2013).
22. V. Ferrando, A. Calatayud, P. Andrés, R. Torroba, W. D. Furlan, and J. A. Monsoriu, IEEE Photon. J. **6**, 1 (2014).
23. J. Ke, J. Zhang, and J. Zhu, Chin. Opt. Lett. **13**, 080501 (2015).
24. J. Ke and J. Zhang, Appl. Opt. **54**, 7278 (2015).
25. J. Zhang, Opt. Express **23**, 30308 (2015).
26. H. Dammann and E. Klotz, Opt. Acta **24**, 505 (1977).
27. C. Zhou and L. Liu, Appl. Opt. **34**, 5961 (1995).
28. C. Zhou, J. Jia, and L. Liu, Opt. Lett. **28**, 2174 (2003).